Nano Energy 59 (2019) 705–714

Contents lists available at ScienceDirect

Nano Energy

journal homepage: www.elsevier.com/locate/nanoen

Full paper

Self-powered implantable electrical stimulator for osteoblasts' proliferation and differentiation

Jingjing Tian[a,b,1], Rui Shi[c,1], Zhuo Liu[d], Han Ouyang[b], Min Yu[e], Chaochao Zhao[b], Yang Zou[b], Dongjie Jiang[b], Jingshuang Zhang[c], Zhou Li[b,f,*]

[a] Central Laboratory, Peking Union Medical College Hospital, Peking Union Medical College and Chinese Academy of Medical Sciences, Beijing, 100730, PR China
[b] Beijing Key Laboratory of Micro-nano Energy and Sensor, Beijing Institute of Nanoenergy and Nanosystems, Chinese Academy of Sciences, Beijing, 100083, PR China
[c] Beijing Laboratory of Biomedical Material, Beijing Institute of Traumatology and Orthopaedics, Beijing Jishuitan Hospital, Beijing, 100035, PR China
[d] Key Laboratory for Biomechanics and Mechanobiology of Ministry of Education, School of Biological Science and Medical Engineering, Beihang University, Beijing, 100083, PR China
[e] School of Stomatology and Medicine, Foshan University, Foshan, 528000, PR China
[f] Center on Nanoenergy Research, School of Physical Science and Technology, Guangxi University, Nanning, 530004, PR China

ARTICLE INFO

Keywords:
Self-powered
Triboelectric nanogenerator
Electrical stimulation
Osteoporosis
Osteoblast

ABSTRACT

Osteoporosis and osteoporosis-related fractures were considered as worldwide diseases and arose wide public concern, the costs for incident osteoporosis-related fractures in United States is nearly $17 billion in 2005 [1], leading to large economic burden. Here, we proposed a self-powered flexible and implantable electrical stimulator, which consisting of a triboelectric nanogenerator (TENG) and a flexible interdigitated electrode. It demonstrated that this self-powered electrical stimulator significantly promoted osteoblasts' attachment, proliferation and differentiation, the level of intracellular Ca^{2+} was up-regulated after electrical stimulation. In addition, the self-powered electrical stimulator was further demonstrated to be driven by the daily movement of a rat, suggesting the practical use as an implantable medical electronic device to electrically induce osteoblasts' differentiation and bone remodeling. Described above, the self-powered electrical stimulator probably could meddle bone homeostasis, alleviate osteoporosis and osteoporosis-related fractures. This work shows great progress not only for TENGs' applications in implantable medical devices but also for clinical therapy of osteoporosis and osteoporosis-related fractures.

1. Introduction

Osteoporosis is a major and global public health problem, the fundamental to the pathophysiology of which is an imbalance between the tightly coupled processes of bone resorption and bone formation [2]. It is reported that there are 16.8 million people in the United States have osteoporosis, and 80% of them are women [3]. Those who have osteoporosis are vulnerable to osteoporotic fracture, it is estimated that the lifetime risk for total osteoporotic fractures of women who have osteoporosis is 45% [4]. Additionally, osteoporosis not only decreased the patients' quality of life significantly, but the mortality following up fracture is doubled and increased constantly [5].

Osteoporosis is a metabolic bone lesions characterized by low bone mass and deterioration of bone tissue, leading to increased bone brittle and prone to fractures of the hip, spine and forearm [6]. The strength and mass of bone lies on the delicate balance between bone resorption by osteoclasts and bone formation by osteoblasts [7]. After age 40 or other diseases such as trauma or tumor, bone destruction exceeds bone formation, resulting in local or systemic bone loss called osteoporosis [8]. So balancing bone resorption and formation is an effective way to treat or alleviate osteoporosis. Nowadays, the therapeutic approaches to osteoporosis are concentrate on inhibiting the formation or activity of osteoclasts, far less attention has been paid on promoting activity of osteoblasts and bone formation.

Bone homeostasis was regulated by a wide variety of systemic and local stimulation, including biochemical and physical factors. Recently, a large number of studies have shown that physical electrical stimulation could enhance osteogenesis and promote bone formation *in vitro* and *in vivo* [9,10], such as direct current [11,12], pulse electric current [13], electric and electromagnetic fields [14–16] et al. However,

* Corresponding author. Beijing Key Laboratory of Micro-nano Energy and Sensor, Beijing Institute of Nanoenergy and Nanosystems, Chinese Academy of Sciences, Beijing, 100083, PR China.
E-mail address: zli@binn.cas.cn (Z. Li).
[1] These authors contributed equally to this work.

https://doi.org/10.1016/j.nanoen.2019.02.073
Received 1 February 2019; Received in revised form 25 February 2019; Accepted 27 February 2019
Available online 06 March 2019
2211-2855/

electrical stimulation has a major drawback of external power consumption, making it hard to meet the demand of miniaturization and weight reduction for implantable and mobile electronic medical devices.

The advent of triboelectric nanogenerator (TENG) provide an effective way to convert mechanical energy of living creature into electric energy [17,18]. Based on the working principle of contact electrification and electrostatic induction, many self-powered electronic medical devices have been developed. It has been reported that TENG was used to collect the breathing energy from mouse to power a pacemaker [19,20]. It also has been studied as a self-powered active pulse sensors [21,22], on account of that the amplitude and frequency of output signals depend on the external mechanical stimulation. And a self-powered wireless transmission device was also systematically studied by harvest the biomechanical energy from rhythmical cardiac contraction and relaxation [23,24]. Moreover, some self-powered electrical stimulation device based on TENG were also explored, such as enhancing the proliferation and migration of fibroblast cells [25] or promoting wound healing [26]. Most interestingly, a weight control device was developed recently via an implanted self-powered vagus nerve stimulation device [27].

Here, we proposed a self-powered flexible and implantable electrical stimulator, which significantly promoted osteoblasts' attachment, proliferation and differentiation. It also demonstrated that the level of intracellular Ca^{2+} was up-regulated after electrical stimulation, and the increase of intracellular Ca^{2+} plays a critical role in regulating osteoblasts' proliferation, differentiation and/or osteogenesis [28–31]. Additionally, the self-powered electrical stimulator was also expected to be applied in an implantable medical electronic device to electrically induce bone formation and healing. This work shows great progress not only for TENGs' applications in implantable medical devices but also for long-term therapy of osteoporosis and bone remodeling.

2. Materials and methods

2.1. Fabrication of the TENG for cell stimulation

Al film (3 × 3 × 0.1 cm) served as both the friction layer and electrode layer of the fabricated TENG, which was washed by ethanol and deionized water three times successively, and then polished by sandpaper to fabricate linear structures (Fig. 1b). The other friction layer of TENG is nanostructured Polytetrafluoroethylene (PTFE) film as shown in Fig. 1c, which was processed by inductively coupled plasma-reaction ion etching (ICP) system (SENTECH/SI 500, Germany). Firstly, PTFE with the thickness of 100 μm and the size of 3 × 3 cm was rinsed consecutively by acetone, ethanol and deionized water three times, respectively. Then PTFE film was blown dry with nitrogen gas to remove any adsorbed moisture. Afterwards, 10 nm Au was sputtered onto the PTFE surface serve as the mask for etching by a sputter coater (Cressington 108Auto, UK) for 60 s. Then, the processed PTFE was etched through ICP reactive ion etching for 300 s. The reaction gas were 15.0 sccm Ar, 10.0 sccm O_2 and 30.0 sccm CF_4. The ICP power were set as 400 W and 100 W, respectively. Subsequently, an ultrathin Au layer with the thickness of 50 nm was deposited on the back surface of nanostructured PTFE by magnetron sputter (Denton Discovery 635, USA), which act as the other electrode of TENG. Two electrode layers were stick on to the surface of acrylic plate, and the spring in the four corners served as the spacer to ensure the contact and separation of friction layers as shown in Fig. 1a.

A linear motor was used to apply a periodical compressive force on TENG at a frequency of 2 Hz. The acceleration and deceleration speed of linear motor were set as 3 m/s^2. The open-circuit voltage was measured by a digital oscilloscope (Keithley DPO6450, USA). The short-current and the quantity of transferred charges were measured by an electrometer (Keithley 6517B, USA).

2.2. Preparation of the interdigitated electrode

Polyethylene terephthalate (PET) with the thickness of 100 μm and the size of 9 × 9 cm was prepared firstly, then rinsed with ethanol for three times, and blown dry with nitrogen gas. Afterwards, photoresist (SUN-115 P, China) was poured on the dried PET, and homogenized by spin coater at 2500 rpm for 25 s, then baked for 1 min at 95 °C immediately. After that, PET with photoresist was exposed by a high-resolution transparency mask containing interdigital pattern for 15 s, then baked for another 1 min at 95 °C immediately, and then immersed it into eikonogen for 15 s and rinsed by deionized water to develop interdigital pattern. Then, Au film with the thickness of 200 nm was sputtered onto the interdigital surface by magnetron sputter. At last, the photoresist and excess Au were stripped by immersed the prepared sample into stripping liquid. Afterwards, the total device was packaged by Polydimethylsiloxane (PDMS) with the thickness of 50 μm using a spin coater at 2500 rpm for 60 s (Fig. 2b).

2.3. Cell culture

The as-prepared interdigitated electrode was fixed on the surface of the 6-well culture plate after sterilization. Then the hollow cylinders with the inside diameter of 4.5 mm similar with 96-well plates (Φ = 3.2 mm) printed by 3D printer were fixed on the interdigitated electrode by PDMS as shown in Fig. S1. Murine calvarial preosteoblasts (MC3T3-E1, ATCC CRL-2594) were used and cultured in α-MEM (Minimum Eagle's Medium) containing 10% fetal bovine serum and 1% penicillin-streptomycin. The MC3T3-E1 cells were seeded in the hollow cylinder (5000 cells/well) and incubated in cell incubator with a humidity atmosphere containing 5% CO_2 at 37 °C. Electrical stimulation was applied 24 h after seeding.

2.4. Electrical stimulation of MC3T3-E1

The self-powered electrical stimulator device was consisted of a TENG, a rectifier and a flexible interdigitated electrode as shown in Fig. 2a, the TENG connected to the interdigitated electrode using a rectifier bridge. Furthermore, the prepared interdigitated electrode was packaged by a thin PDMS film to avoid electrochemical reaction between electrodes and culture medium. The cells were seeded in the hollow cylinders that fixed on the interdigitated electrode. The electrical energy converted from the mechanical energy of a linear motor or the daily movement of rat by TENG served as the energy source and provide the electric field (EF) that apply to cells. The EF stimulation was applied 24 h after seeding, and the cells were stimulated for 1 h per day. The group that without EF treatment served as control group.

2.5. Statistical analysis of cell attachment

To investigate the effect of EF stimulation on cell attachment and spreading area, after cultured and stimulated for 1, 3 and 6 h, the MC3T3-E1 cells were imaged by immunofluorescence staining of F-action and nuclei. After washing with PBS three times, MC3T3-E1 cells were fixed with 4% paraformaldehyde solution for 15 min at room temperature, then washing with PBS for three times again. After that, cells were incubated with phalloidin solution for 30 min and DAPI solution for 5 min to stain the F-action and nuclei, then washing with PBS for three times. Finally, the stained cells were characterized using an inverted fluorescence microscope. For the statistical analysis of cell attachment, the relative average quantity of attached cells and total cell attachment areas of ten images were counted and calculated by Image-Pro Plus software.

2.6. Characterization of proliferation

MTT [3-(4,5-dimethyl-2-thiazolyl)-2,5-diphenyl-2-H-tetrazolium

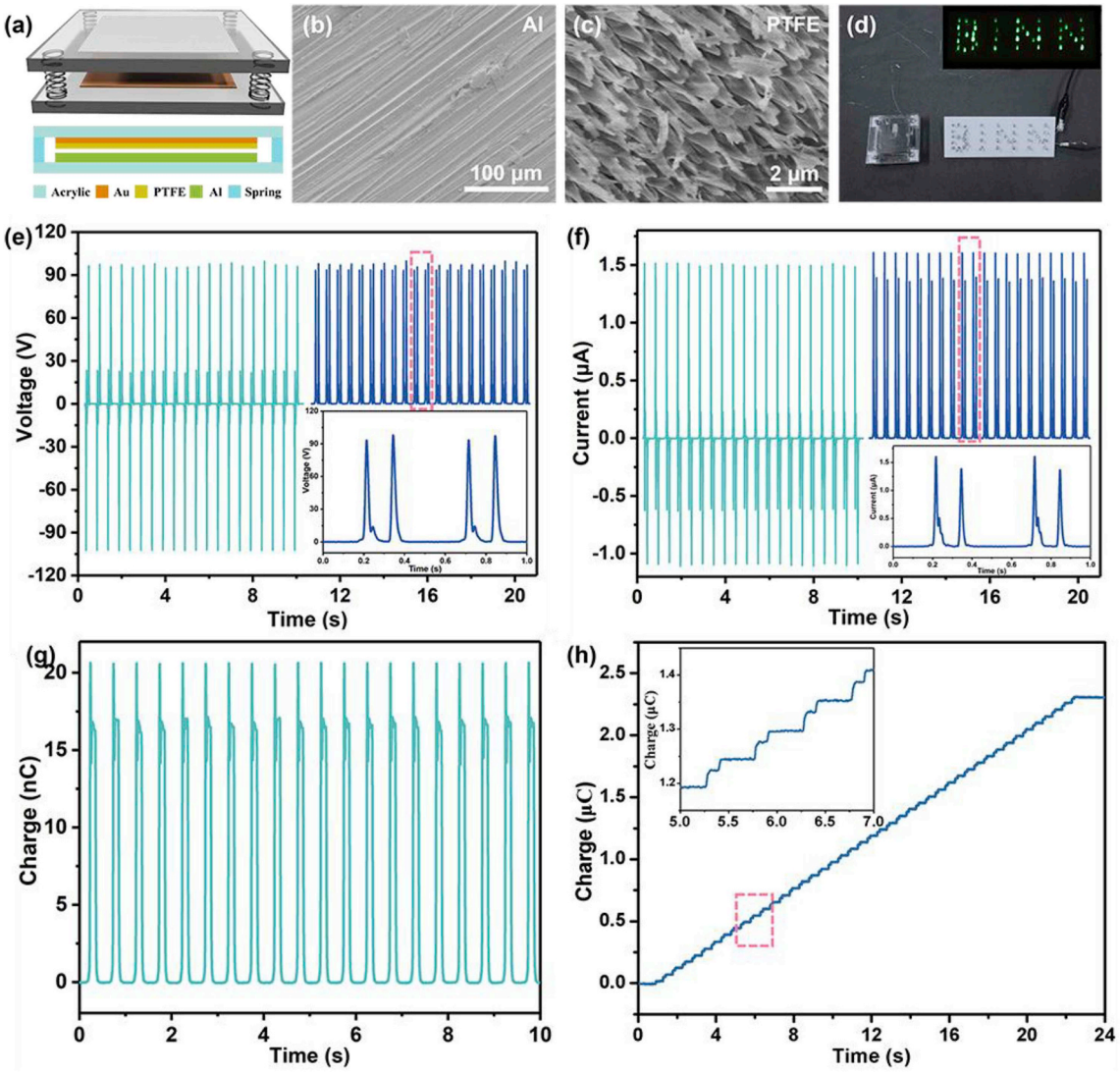

Fig. 1. The structure and output performance of TENG. (a) Schematic diagram of TENG that used for cell stimulation *in vitro*. (b, c) SEM images of the linear microstructures on Al film and nanostructures on PTFE film, the obtained nanostructured arrays on PTFE were dense and homogeneous, with an average height of about 100 nm. (d) Photograph of the lighting panel of forty green LEDs driven by the TENG. (e) The output voltage of TENG driven by a linear motor with and without rectification, the insert image is the enlarge photograph of output voltage with rectification (refer to the dashed line). (f) The output current of TENG with and without rectification, the insert image is the enlarge photograph of the output current after rectified (refer to the dashed line). (g) The transferred charge of TENG without rectification. (h) The transferred charge of TENG after rectified. The insert image is the enlarge photograph in the dashed line.

bromide] assay was used to quantitatively evaluate the cell proliferation level, and cells were stimulated for 1 h per day. 24 h after EF stimulated for 1, 3, 5 days, the culture medium was replaced by 200 μL fresh α-MEM, then 10 μL MTT (0.5 mg/mL in final concentration) was added to the fresh culture medium. After MC3T3-E1 cells incubated in the cell incubator for 4 h, the culture supernatant was removed, and 200 μL dimethylsulfoxide (DMSO) was added to dissolve the formed formazan crystals. After shaking in dark for 5 min, the quantity of dissolved formazan crystals (representing viable cells) was assayed at 490 nm by an enzyme linked immunosorbent assay (ELISA) reader. Four parallel replicates for each group were measured.

2.7. Analysis of alkaline phosphatase (ALP)

Extracellular ALP level was detected after EF stimulated for 1, 6, 12 and 18 days as shown in Fig. S3. Cells were cultured in the hollow cylinders with the inside diameter of 15.6 mm similar with 24-well plates printed by 3D printer, and cells were stimulated for 1 h per day. 24 h after EF stimulated for 1, 6, 12 and 18 days, MC3T3-E1 cells were fixed with 4% paraformaldehyde solution for 15 min at room temperature, then washed with PBS for three times. After that, 200 μL (enough to coat the cells) BCIP/NBT solution was added and incubated with MC3T3-E1 cells for 20 min at room temperature. At last, cells were rinsed with deionized water three times and examined microscopically. Afterwards, the gray values of image that dyed by BCIP/NBP were calculated by Image-Pro Plus to reflect the extracellular ALP level.

2.8. Measurement of intracellular Ca^{2+}

Ca^{2+} sensitive fluorescent dye Fluo-4 AM ester stock solution with 1 mM was used to measure the level of intracellular Ca^{2+}. Fluo-4 AM ester stock solution was diluted to 5 μM for use firstly. EF stimulation was immediately after cell seeding, and intracellular Ca^{2+} level was measured 20, 40 and 60 min after EF stimulation. After certain stimulation time, the culture medium was removed firstly, and PBS solution was used to rinse MT3T3-E1 cells for three times. After that, 100 μL diluted Fluo-4 AM ester solution was added and incubated with MT3T3-E1 cells for 40 min at 37 °C. Subsequently, Fluo-4 AM ester solution was

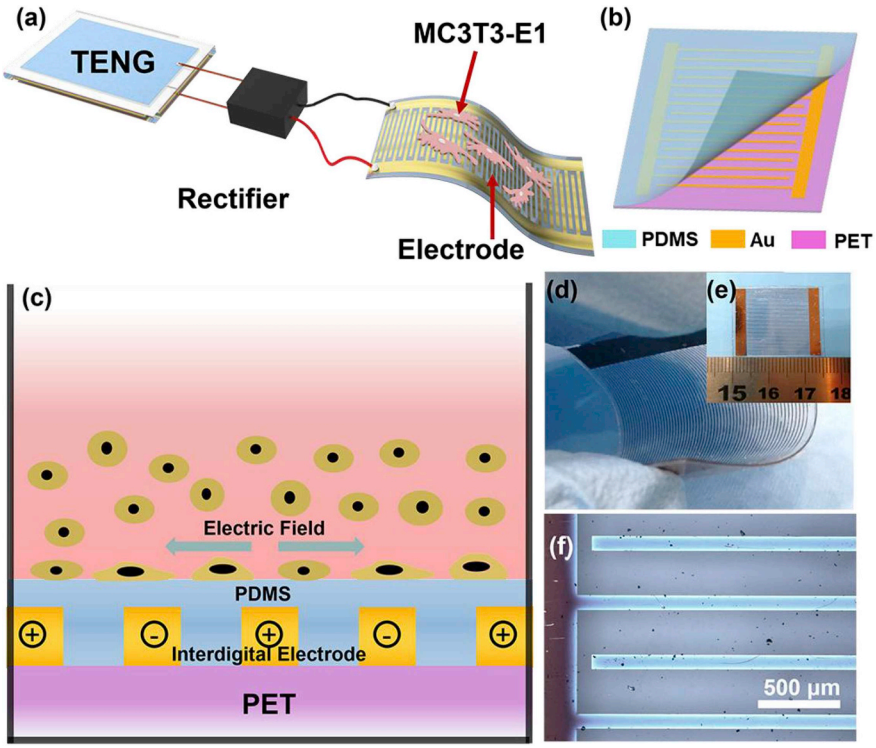

Fig. 2. The schematic diagram of interdigitated electrode and the self-powered electrical stimulator. (a) The schematic diagram of cell stimulation device, which consisting of a TENG, a rectifier and a flexible interdigitated electrode. (b) The fabricated interdigitated electrode employed PET as substrate and packaged by PDMS. (c) The sedimentation and adhesion process of MC3T3-E1 cells under electric field stimulation on the packaged interdigitated electrode. (d, e) The flexibility and the size of the interdigitated electrode after package *in vitro*. (f) Optical image of the interdigitated electrode acquired by metal graphic microscope, which shown that the width of the electrode is 100 μm and the distance between two adjacent electrodes is 300 μm.

removed, and MT3T3-E1 cells were detached by 0.25% trypsin/EDTA. Then the mixture was centrifuged for 5 min at 3000 rpm/min, and the acquired supernatant was discarded. Finally, cells were washed for three times and resuspended by 100 μL PBS, Flow Cytometer was used to measure the fluorescence intensity at the excitation wavelength of 488 nm.

2.9. Implantation and electrical measurement of TENG in vivo

The Sprague Dawley (SD) rats (200g, the Academy of Military Medical Sciences, China) was used in the *in vivo* experiment. The SD rat was anesthetized by intake of isoflurane gas (1–3% in pure medical grade oxygen) firstly, and followed by intraperitoneal injection of pentobarbital sodium (30 mg/kg) for anesthesia maintenance. All the implantation operations were performed strictly in accordance to "Beijing Administration Rule of Laboratory Animals" and the national standard "Laboratory Animal Requirements of Environment and Housing Facilities (GB 14925–2001)". The flexible ITO was employed as the friction and electrode layer of implanted TENG instead of Al film (Fig. 6a). Then the TENG was encapsulated in PDMS with the thickness of 50 μm and cut into the size of 2.0 cm × 2.0 cm (Fig. 6b) before implantation since the animal is small. To confirm the TENG can output well *in vivo* under the drive of daily movement of Srat, the fabricated TENG was implanted in the surface of femur region. The wound was instantly sutured after implantation. To simulate the daily movement of SD rat, a linear motor was used to gently pull the leg of the rat through a line (Fig. 6d), the pulling force was about 0.5 N with 1 Hz. The generated electrical output performance was recorded by a digital oscilloscope system (Keithley DPO6450, USA) and an electrometer (Keithley 6517B, USA).

3. Results and discussions

The as-fabricated self-powered electrical stimulator is composed of a TENG, a rectifier and a flexible interdigitated electrode. The TENG used for MC3T3-E1 stimulation *in vitro* was consists of two friction layers and electrode layers as shown in Fig. 1a, Al and PTFE films served as friction layers. Those two materials have distinctly different triboelectric characteristics with PTFE film easy to gain electrons and Al film easy to lose electrons. A layer of Au (50 nm) was deposited on the back of PTFE served as one electrode, and Al film itself served as another electrode. To improve the output performance of the TENG, Al film was polished by sandpaper to produce linear micro-structures [32] (Fig. 1b). At the same time, PTFE thin film was processed by ICP to obtain nanostructure arrays (Fig. 1c), which could enlarge the effective contact area and enhance the contact electrification [33]. The obtained nanostructure arrays were dense and homogeneous, with an average height of about 100 nm. Furthermore, acrylic plate served as the substrate material to avoid the damage of linear motor on friction and electrode layers, and springs in four corners were used to ensure the contact and separation of two friction layers.

The working principle of TENG was previously reported and is based on the coupling of contact electrification and electrostatic induction [34,35]. When the external force is applied, two friction layers were touched and rubbed with each other, hence, triboelectric charges with opposite signs were generated and distributed on the surface of two friction layers, resulting in net negative charges on the surface of nanostructured PTFE film and net positive charges on micro-structured Al film, respectively. When the external force is released, in order to balance the electric potential difference established by the tribocharges on the micro-structured Al film and nanostructured PTFE film, the electrons in the attached Au induction electrode and micro-structured Al will be driven to flow back and forth through the external circuit, thus generate an electrical signal modulated by the external force. Therefore, with repeated applying and releasing of the external force, electrons are driven flow through the external load in an alternating manner.

The output performance of TENG are important to the EF stimulation of cells. A linear motor with a constant vertically compressive force was applied to the fabricated TENG, and the output performance was measured simultaneously as shown in Fig. 1e–h. The output voltage, current and transferred charge without rectified were about 100 V, 1.5 μA, and 21 nC, respectively (Fig. 1e, f, g), and the power is enough to light forty green LEDs simultaneously (Fig. 1d). Additionally, the

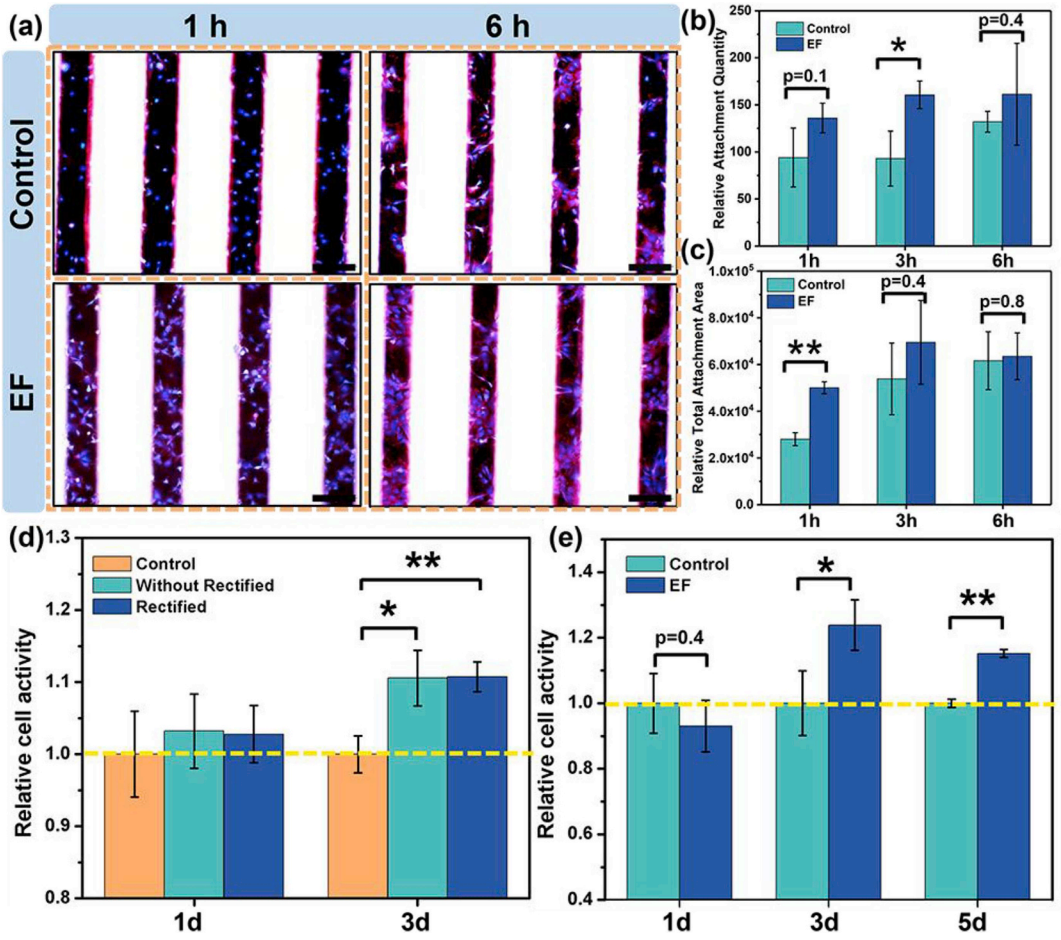

Fig. 3. The morphology and the proliferation of MC3T3-E1. (a) Quantity and morphology of MC3T3-E1 cells after seeded for 1 and 6 h with and without EF stimulation, MC3T3-E1 was stained by phalloidin (red) and DAPI (blue). Scale bar: 200 μm. (b) The relative quantity of attached MC3T3-E1 cells after stimulated for 1, 3 and 6 h, there were 44.68%, 72.76% and 22.22% higher than no treatment group, respectively. (*$p < 0.05$, $n = 10$). (c) The relative total attachment areas of MC3T3-E1 cells after stimulated for 1, 3 and 6 h. The EF treatment group were 78.37%, 29.05% and 3.06% greater than control group (**$p < 0.01$, $n = 10$). (d) The comparison of cell proliferation between rectified and no rectified groups after stimulated for 1 and 3 days. (e) The MTT results showed the proliferation of MC3T3-E1 after EF stimulated for 1, 3 and 5 days after rectified. The MC3T3-E1 cells were proliferated 23.82% and 15.18% higher than control group after stimulated for 3 and 5 days, respectively. Two sample *t*-test was used to examine data, and significance was determined at × *$p < 0.05$, **$p < 0.01$, $n = 4$.

voltage, current and transferred charge after rectified were also recorded. From the right part of Fig. 1e and f and their enlarge graphs we can see that the TENG output an open-circuit voltage of 100 V and a short-circuit current of about 1.6 μA. As shown in Fig. 1h and its enlarge graphs, the transferred charge was around 2.2 μC within 23 s' charge after rectified.

Electrical stimulation has been used in the treatment of lots of conditions [25–27], and a great number of researches proved the feasibility and effectiveness of electrical stimulation on bone regeneration in clinical and research settings [36,37]. Hence, electrical stimulation offers a promising way for fracture healing and bone repairing [38,39]. As we known that the electrical output of TENG characterized by high voltage and low current, which were propitious to the electrical stimulation in the bone regeneration and repair field. Here, a self-powered electrical stimulator was proposed and shown in Fig. 2a, which consisted of a TENG, a rectifier and a flexible interdigitated electrode. The interdigitated electrode employed PET as substrate, and the entire device was packaged by a flexible PDMS layer with the thickness of 50 μm to maintain the good flexibility and enhance the stability of the whole device (Fig. 2b, d). After that, the packaged interdigitated electrode device was cut into the size of 2.5 × 2.5 cm as shown in Fig. 2e. The width of the electrode in interdigitated electrode device is 100 μm, the distance between two adjacent electrodes is 300 μm (Fig. 2f). Considering the thickness of the PDMS package layer, the actual strength of electric field (EF) at the interface between the MC3T3-E1 cells and device was about 150 V/cm, and the stimulate depth was about 250 μm, which were calculated by finite element simulation (Fig. S1, supporting information).

As for the electrical stimulation experiment, MC3T3-E1 was chosen as model cell to provide solid support for bone tissue regeneration application of the fabricated self-powered electrical stimulator. As we known that pulsed DC stimulation and biphasic pulse stimulation all have shown effective for bone regeneration [40–42]. Therefore, the effect of alternating current (AC, without rectified) and pulsed direct current (DC, rectified) signals on cell proliferation were detected by MTT assay firstly as shown in Fig. 3d, there are almost no significant difference between control and stimulation groups after EF stimulated for 1 day. But after 3 days' EF stimulation, AC and pulsed DC stimulation group were proliferated 10.56% ($p < 0.05$, $n = 4$) and 10.75% ($p < 0.01$, $n = 4$) higher than control group, and all have significant difference. However, considering that pulsed DC stimulation has been reported that it has the potential to promote beating rates of the cardiomyocyte clusters significantly [35], and it also could stimulate the neurons grow parallel to the EF orientation obviously [43], hence we adopt the pulsed DC signal to stimulate MC3T3-E1 in all the following experiment sets.

As shown in Fig. 2c, cell attachment and spreading were happened immediately after seeding, the cell adhesion process and cell

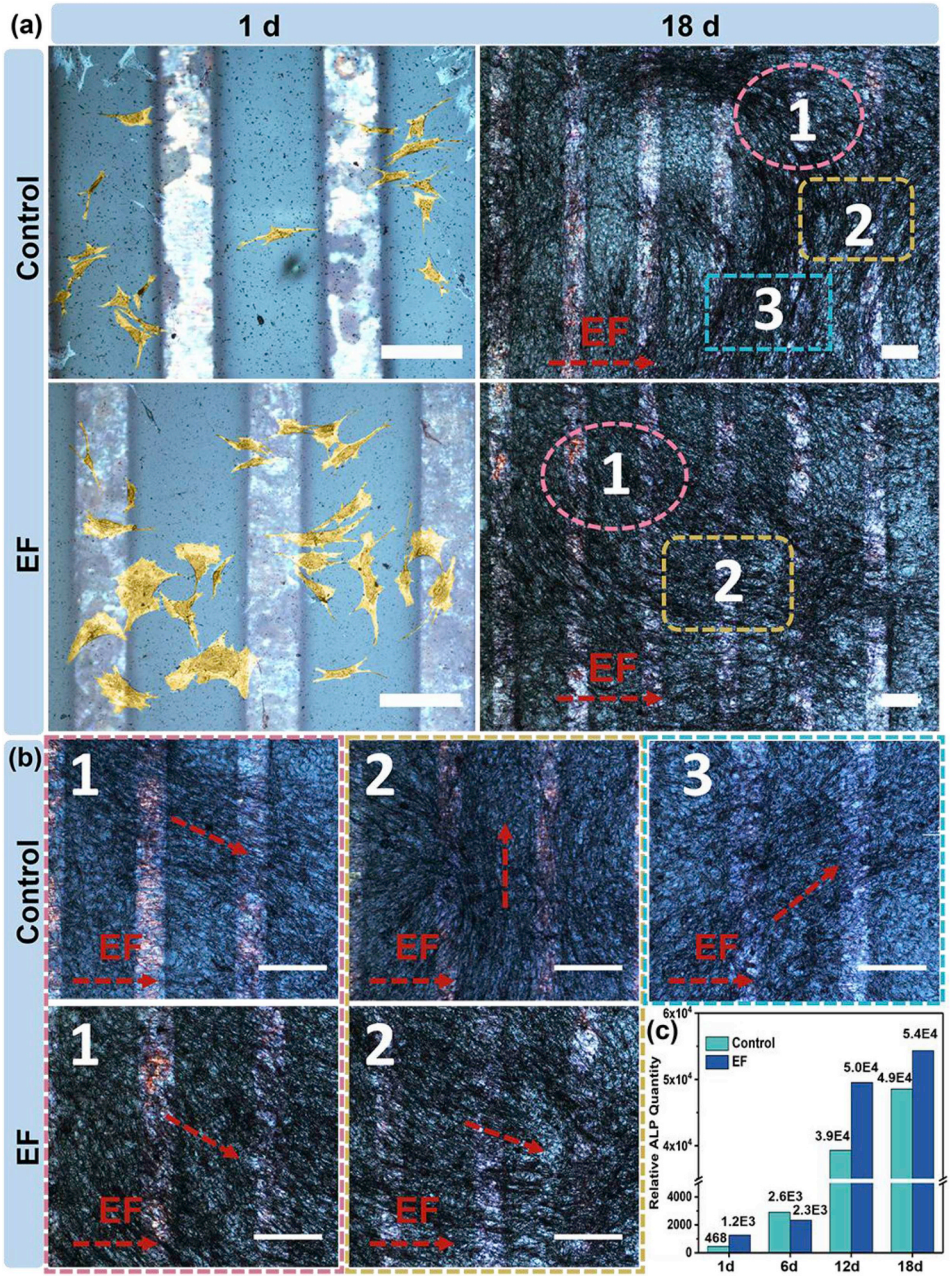

Fig. 4. The extracellular ALP level that dyed by BCIP/NBP after EF stimulated for various time. (a) ALP level implied by BCIP/NBP staining (grayish black) after stimulated for 1 and 18 days. (b) The enlarged view of BCIP/NBP staining images after 18 days of EF stimulation, which showed the orientation and distribution of MC3T3-E1 were nearly parallel to the EF orientation, but the control group have no consistent orientation with EF orientation. (c) The relative ALP level stem from the gray value of images that dyed by BCIP/NBP, and the gray value of EF treatment group was 28.2% and 10.2% higher than the control group after 12 and 18 days of EF stimulation. Scale bar: 200 μm.

morphologies may be influenced by EF stimulation. Hence, the cell adhesion process after seeding including morphologies and spreading areas were detected after EF stimulated for 1, 3 and 6 h (Fig. 3a–c). EF stimulation was performed immediately after seeding, and after stimulated for 1, 3 and 6 h, the cell cytoskeleton and nucleus were stained red and blue by phalloidin and DAPI, respectively. The immunofluorescent staining images revealed the normal adhesion process of MT3T3-E1 after seeding, and from the statistical analysis of the quantity of attached cells and total attachment areas (Fig. 3b and c) we can conclude that EF stimulation could promote the cell spreading and adhesion process. Compared with no EF treatment group, the EF treated group attached more earlier and cell spreading areas were generally greater (Fig. 3a). From the statistical analysis results, we earned that the quantity of attached cells were 44.68%, 72.76% and 22.22% higher than no treated group after EF stimulated for 1, 3 and 6 h, respectively. Furthermore, the total spreading areas were 78.37%, 29.05% and 3.06% greater after 1, 3 and 6 h of EF stimulation, respectively. It illustrated that the difference between these two groups decreased along with time, because all cells would normally attach at last, but EF stimulation could speed up the process.

Additionally, from the statistical analysis results of the quantity of attached cells and total attachment areas, we also learned that compare to control group, the total attachment areas have significant difference after 1 h of EF stimulation and the quantity of attached cells have significant difference after 3 h of EF stimulation. It may because that the cells enter the spreading process firstly after seeding, and EF stimulation can promote cell adhesion and spreading, leading to the total attachment areas of cells have significant difference after 1 h of EF stimulation. However, 3 h after seeding, most cells finished their adhesion process in EF stimulation group, but not in control group, resulting in the quantity of attached cells have significant difference after 3 h of EF stimulation. From the above, we can indicate that EF stimulation can significantly influence the spreading area and morphology of MC3T3-E1 immediately after seeding.

After cell adhesion, MC3T3-E1 cells started their proliferative activity. Therefore, cell viability and proliferation of MC3T3-E1 cells were

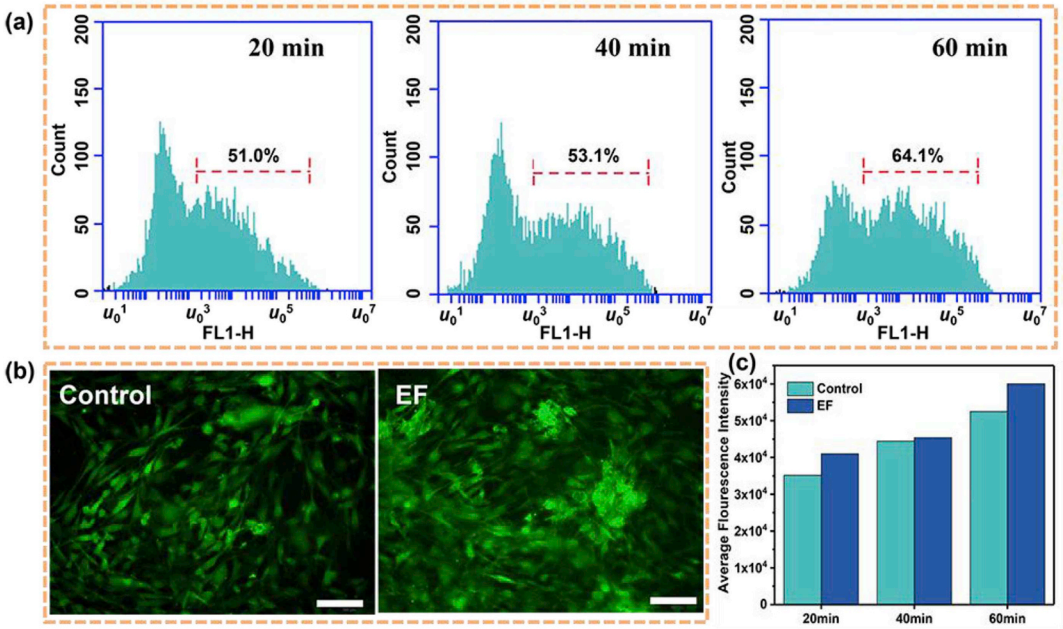

Fig. 5. The intracellular Ca^{2+} level of MC3T3-E1 cells, which was quantitatively measured by flow-cytometer after different stimulation time of EF. (a) The percentage of Ca^{2+} positive cells after EF stimulated for 20, 40 and 60 min, they were obtained based on a uniform intensity threshold set according to the 20 min of EF stimulation group. (b) The optical fluorescence diagrams of MC3T3-E1 cells dyed by Fluo-4 AM after EF stimulated for 60 min. Scale bar: 200 μm. (c) The average fluorescence intensity acquired from average FL1-H intensity by flow-cytometer.

quantitatively investigated by MTT assay, and the stimulation time was extended to 5 days as shown in Fig. 3e, the MC3T3-E1 cells have no proliferation trend on day 1, and there was almost no difference between EF stimulation and control group. On day 3 and day 5, the cell number of EF stimulation group was significantly higher than that of control group. Specifically, cell viability of EF stimulation group was 23.82% ($p < 0.05$, $n = 4$) and 15.18% ($p < 0.01$, $n = 4$) higher than that of control group after 3 and 5 days of EF stimulation. However, the growth ratio of cell viability on day 5 was lower than that of day 3, it may attribute to that some cells have entered the stagnate phase of cell proliferation. The results indicated that the self-powered electrical stimulator could promote cell proliferation significantly.

After that, the differentiation of MC3T3-E1 cells was detected by measure the extracellular Alkaline phosphatase (ALP) level. ALP is an important early phenotypic marker for the bone matrix synthesis and the maturity of the extracellular matrix of MC3T3-E1 cells, which could be used to detect cell differentiation degree and early bone matrix formation [44]. Therefore, ALP was stained by BCIP/NBP to evaluate osteogenic differentiation degree after the stimulation of self-powered electrical stimulator. EF treatments of 150 V/cm at 2 Hz was applied for 1 h per day. As shown in Fig. 4a and b, ALP positive cells were dyed with distinct grayish black. After stimulated for 1 day (Fig. 4a), hardly any ALP was found, but we can see the different morphologies of MC3T3-E1 between control and EF stimulation group. It shown that the cells in EF treatment group were spreading fully, and the spreading areas were much greater than control group, which in agreement with previous cell attachment results. After 18 days of culturing (Fig. 4b, the enlarge view of Fig. 4a that cultured for 18 days), most of the electrically stimulated MC3T3-E1 cells were well arranged and oriented, MC3T3-E1 cells were nearly parallel to the EF orientation obviously. Whereas, the cell arrangement in the control group had no obvious orientation. Furthermore, the extracellular ALP level after EF stimulated for 6 and 12 days were also examined as shown in Fig. S3. To further investigate the osteogenic differentiation degree, the extracellular ALP was quantitatively detected by calculate the gray value of images that dyed by BCIP/NBT (grayish black, Fig. S2 and Table S1, supporting information) using Image-Pro Plus software. As shown in Fig. 4c, the ALP level has no clear distinction between EF and control group after stimulated for 1 or 6 days. On day 12, the ALP level of MC3T3-E1 cells in all samples increased dramatically with the gray value was increased an order of magnitude than that of cells on day 6. However, after stimulated for 18 days, the relative ALP level in EF stimulation group increased slightly, while there has an apparently increase in control group. This may due to that ALP is an early marker of osteogenic differentiation. Specifically, the gray values (representing ALP level) of EF treatment group were 28.2% and 10.2% higher than the control group after stimulated for 12 and 18 days, respectively. The increased ALP level implied that the bone matrix synthesis was activated by EF stimulation and the MC3T3-E1 cells had a more mature extracellular matrix after EF treatment.

We have proved the active role of EF stimulation on regulate the adhesion, proliferation and differentiation of MC3T3-E1, but how does it work was not clear yet. It was reported that Ca^{2+} plays a critical role in regulating osteoblast proliferation and/or differentiation via either activation of the calcium sensing receptors and/or increasing the Ca^{2+} influx into osteoblast [28]. And EF stimulation can activate the electrically sensitive Ca^{2+} signal transduction [45]. Therefore, intracellular Ca^{2+} level of MC3T3-E1 cells treated by our self-powered electrical stimulator was further measured by flow cytometry after various stimulation time as shown in Fig. 5. The fluorescence intensity and the percentage of Ca^{2+} positive cells (Fig. 5a) of MC3T3-E1 were obtained and calculated after dyed by Fluo-4 AM (Fig. 5b and c). As shown in Fig 5a, 20 min after EF stimulation, there were about 51.0% Ca^{2+} positive MC3T3-E1 cells, and it increased with stimulation time, which up to 64.1% after EF stimulated for 60 min. This may because that EF stimulation of our self-powered electrical stimulator can activate the electrically sensitive Ca^{2+} signal transduction, leading to the activation of the calcium sensing receptors and/or increasing the Ca^{2+} influx into MC3T3-E1 cells. Additionally, the average fluorescence intensity of intracellular Fluo-4 (representing Ca^{2+} level) was recorded immediately after EF stimulation. Fig. 5b shows the fluorescence intensity intuitively after EF stimulated for 60 min. Comparing with control group, the fluorescence intensity was increased obviously after EF stimulation. Furthermore, quantitatively analysis of the average

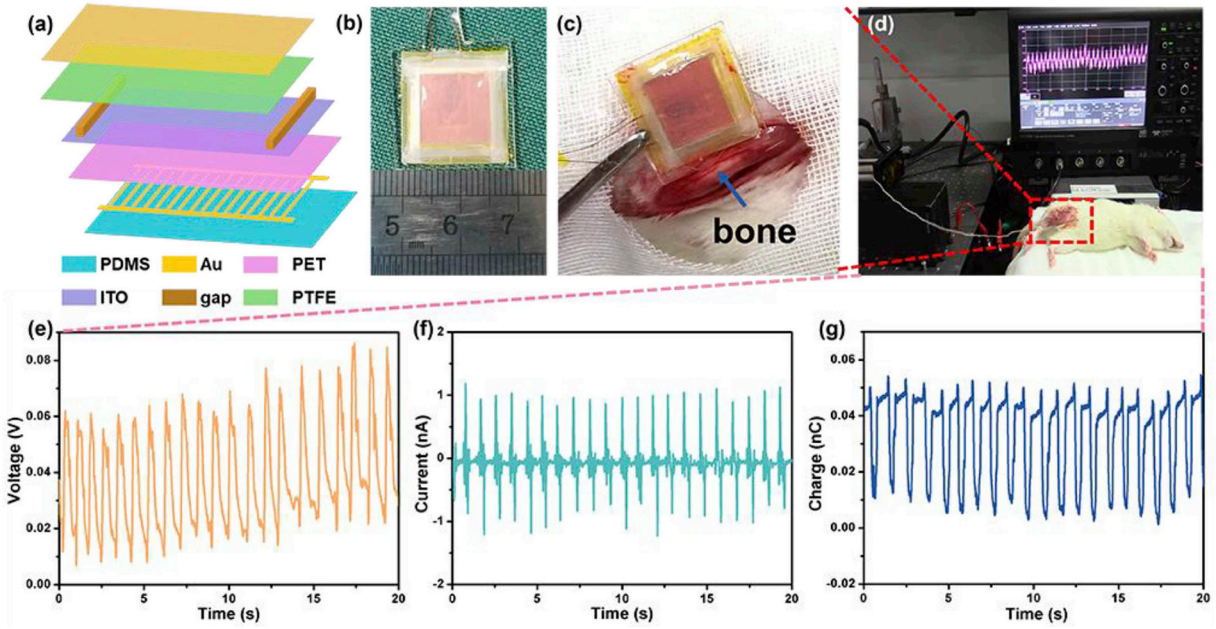

Fig. 6. The intending self-powered implantable stimulator electrically induced bone formation and healing. (a) The implantable self-powered electrical stimulator consisting of a flexible TENG and a flexible interdigital stimulator. (b) The size of implanted TENG was strictly limited to 2.0 cm × 2.0 cm after package. (c) The surface of femur region that the flexible TENG implanted. (d) Image of the output measurement process, a linear motor was used to pull the leg of SD rat through a line. The open-circuit voltage (e), short-circuit current (f) and transferred charge (g) were reached to around 60 mV, 1 nA and 0.04 nC *in vivo*, respectively.

fluorescence intensity of Fluo-4 also shown the higher Ca^{2+} level after EF stimulation by flow cytometry (Fig. 5c), which illustrated the active of Ca^{2+} signaling by EF stimulation. Therefore, those results provide solid evidence for that EF stimulation modulate cell adhesion, proliferation and differentiation may through calcium ion channels related pathway by up-regulating cytosolic Ca^{2+}.

In addition, to demonstrate the potential of practical use of the self-powered electrical stimulator, we implanted the flexible TENG in living creatures. As shown in Fig. 6a, PTFE and indium tin oxide (ITO) were selected as friction layers instead of Al film to maintain the flexibility of the whole device, TENG and interdigitated electrode were expected to integrate and stack together, connecting by a rectifier and a capacitor acting as an electricity reservoir. Then the integrated TENG and interdigitated electrode were packaged by a thin flexible PDMS layer (50 μm) to enhance the structural stability and avoid tissue fluid permeation. Afterwards, the possibility of practical use of the self-powered electrical stimulator was verified by implanting the flexible TENG in bone surface, and the output of implanted TENG was measured. The size of implanted TENG after package was strictly limited to 2.0 cm × 2.0 cm (Fig. 6b), since the output of TENG was distinctly affected by the size of implanted TENG and the external driving force, so the output performance was limited by the small animal. Then the fabricated flexible TENG was implanted in the surface of femur region of SD rat as shown in Fig. 6c, the wound was instantly sutured after implantation. In the output measurement process, the daily movement of rats was mimicked by pull the leg of SD rat using a linear motor through a line (Fig. 6d). The pulling action conducts a regular motion of leg, which extruded the TENG periodically and produced electric energy (video S1, supporting information). Then the electric energy can be stored in a capacitor to drive interdigital stimulator periodically. As shown in Fig. 6e–g, the output of the implanted TENG *in vivo* was clearly identified, the open-circuit voltage, short-circuit current and the transferred charge were reached to around 60 mV, 1 nA and 0.04 nC, respectively. The results indicated that the self-powered electrical stimulator can implant in the surface of bone implants or the fracture region and generate electric energy through the rat's daily activity to stimulate cell activity, which also illustrated the potential of practical applications *in vivo* of our self-powered electrical stimulator.

Supplementary video related to this article can be found at https://doi.org/10.1016/j.nanoen.2019.02.073.

4. Conclusions

In summary, we developed an implantable self-powered electrical stimulator for promoting bone formation, which consist of a flexible TENG, a rectifier and a flexible interdigitated electrode. It was demonstrated that this self-powered electrical stimulator with excellent output can promote the adhesion, proliferation, differentiation of osteoblast progenitor cells and upregulate calcium ion in them. Specifically, it enhanced the attached number of MC3T3-E1 cells by 72.76% after 3 h of stimulation, and increased the total spreading area by 78.37% after 1 h of stimulation. Furthermore, the proliferation of MC3T3-E1 was promoted by 23.82% after 3 days of stimulation and the cells' differentiation level was promoted by 28.2% after 12 days of stimulation. In addition, we implanted the flexible TENG into the surface of the SD rat's femur and found that TENG could convert the mechanical energy of daily movement of rats into electric energy successfully. These results not only pave the way for the future use of TENG in situ stimulation of osteoblasts and other electrically responsive cells such as neurons or muscle cells, but also for the clinical therapy of bone fracture and bone remodeling after bone transplantation.

Acknowledgements

The authors thank the support of National Key R&D Project from Minister of Science and Technology, China (2016YFA0202703), National Natural Science Foundation of China (No. 61875015, 31571006, 81601629, 21801019, 51673029 and 61501039), the Beijing Natural Science Foundation (2182091), China Postdoctoral Science Foundation (2018M641148), Beijing Council of Science and Technology (Z181100004418004) and the National Youth Talent Support Program.

Appendix A. Supplementary data

Supplementary data to this article can be found online at https://doi.org/10.1016/j.nanoen.2019.02.073.

References

[1] R. Burge, B. Dawson-Hughes, D.H. Solomon, J.B. Wong, A. King, A. Tosteson, J. Bone Miner. Res. 22 (2007) 465–475.
[2] M. Chorev, R. Dresnerpollak, Y. Eshel, M. Rosenblatt, Biopolymers 37 (1995) 367–375.
[3] R. Karen, Am. J. Nurs. 111 (2011) 36–37.
[4] G.A. Rodan, T.J. Martin, Science 289 (2000) 1508–1514.
[5] B. Abrahamsen, S.T. Van, R. Ariely, M. Olson, C. Cooper, Osteoporos. Int. 20 (2009) 1633–1650.
[6] M. Priemel, C. von Domarus, T.O. Klatte, S. Kessler, J. Schlie, S. Meier, N. Proksch, F. Pastor, C. Netter, T. Streichert, K. Puschel, M. Amling, J. Bone Miner. Res. 25 (2010) 305–312.
[7] C.M. Karner, F.X. Long, Cell. Mol. Life Sci. 74 (2017) 1649–1657.
[8] L.C. Johnson, R.W. Johnson, S.A. Munoz, G.R. Mundy, T.E. Peterson, J.A. Sterling, Bone 48 (2011) 141–151.
[9] K.E. Hammerick, J. Awhuang, Tissue Eng. 16 (2010) 917–931.
[10] D. Kaynak, R. Meffert, M. Günhan, O. Günhan, J. Periodontol. 76 (2005) 2194–2204.
[11] C.T. Brighton, P. Shaman, R.B. Heppenstall, E.J. Jr, S.R. Pollack, Z.B. Friedenberg, Clin. Orthop. Relat. Res. NA (1995) 223–234.
[12] B.M. Isaacson, L.B. Brunker, A.A. Brown, J.P. Beck, G.L. Burns, R.D. Bloebaum, J. Biomed. Mater. Res. B 97B (2015) 190–200.
[13] B.Y. Yang, T.C. Huang, Y.S. Chen, C.H. Yao, Evid-Based Compl. Alt. 2013 (2013) 607201.
[14] L. Khatib, D.E. Golan, M. Cho, FASEB J. 18 (2004) 1903–1905.
[15] M.T. Tsai, H.S. Chang, K. Chang, R.J. Hou, T.W. Wu, Bioelectromagnetics 28 (2010) 519–528.
[16] C.C. Clark, W. Wang, C.T. Brighton, J. Orthop. Res. 32 (2014) 894–903.
[17] W. Tang, J.J. Tian, Q. Zheng, L. Yan, J.X. Wang, Z. Li, Z.L. Wang, ACS Nano 9 (2015) 7867–7873.
[18] G.Q. Gu, C.B. Han, J.J. Tian, C.X. Lu, C. He, T. Jiang, Z. Li, Z.L. Wang, ACS Appl. Mater. Interfaces 9 (2017) 11882–11888.
[19] Q. Zheng, B.J. Shi, F.R. Fan, X.X. Wang, L. Yan, W.W. Yuan, S.H. Wang, H. Liu, Z. Li, Z.L. Wang, Adv. Mater. 26 (2014) 5851–5856.
[20] Y. Ma, Q. Zheng, Y. Liu, B.J. Shi, X. Xue, W.P. Ji, Z. Liu, Y.M. Jin, Y. Zou, Z. An, W. Zhang, X.X. Wang, W. Jiang, Z.Y. Xu, Z.L. Wang, Z. Li, H. Zhang, Nano Lett. 16 (2016) 6042–6051.
[21] D.Y. Park, D.J. Joe, D.H. Kim, H. Park, J.H. Han, C.K. Jeong, H. Park, J.G. Park, B. Joung, K.J. Lee, Adv. Mater. 29 (2017) 1702308.
[22] H. Ouyang, J.J. Tian, G.L. Sun, Y. Zou, Z. Liu, H. Li, L.M. Zhao, B.J. Shi, Y.B. Fan, Y.F. Fan, Z.L. Wang, Z. Li, Adv. Mater. 29 (2017) 1703456.
[23] D.H. Kim, H.J. Shin, H. Lee, C.K. Jeong, H. Park, G.-T. Hwang, H.-Y. Lee, D.J. Joe, J.H. Han, S.H. Lee, J. Kim, B. Joung, K.J. Lee, Adv. Funct. Mater. 27 (2017) 1700341.
[24] Q. Zheng, H. Zhang, B.J. Shi, X. Xue, Z. Liu, Y.M. Jin, Y. Ma, Y. Zou, X.X. Wang, Z. An, W. Tang, W. Zhang, F. Yang, Y. Liu, X.L. Lang, Z.Y. Xu, Z. Li, Z.L. Wang, ACS Nano 10 (2016) 6510–6518.
[25] W. Hu, X. Wei, L. Zhu, D. Yin, A. Wei, X. Bi, T. Liu, G. Zhou, Y. Qiang, X. Sun, Z. Wen, Y. Pan, Nanomater. Energy 57 (2019) 600–607.
[26] Y. Long, H. Wei, J. Li, G. Yao, B. Yu, D. Ni, A.L. Gibson, X. Lan, Y. Jiang, W. Cai, X. Wang, ACS Nano 12 (2018) 12533–12540.
[27] G. Yao, L. Kang, J. Li, Y. Long, H. Wei, C.A. Ferreira, J.J. Jeffery, Y. Lin, W. Cai, X. Wang, Nat. Commun. 9 (2018) 5349.
[28] M. Zayzafoon, J. Cell. Biochem. 97 (2006) 56–70.
[29] L. Khatib, D.E. Golan, M. Cho, FASEB J. 18 (2004) 1903–1905.
[30] S.T. Li, J. Hu, G. Zhang, W. Qi, P. Zhang, P.F. Li, Y. Zeng, W.F. Zhao, Y.H. Tan, J. Cell. Physiol. 230 (2015) 2164–2173.
[31] M. Zayzafoon, J. Cell. Biochem. 97 (2006) 56–70.
[32] L.M. Zhao, Q. Zheng, H. Ouyang, H. Li, L. Yan, B.J. Shi, Z. Li, Nanomater. Energy 28 (2016) 172–178.
[33] H.S. Wang, C.K. Jeong, M.H. Seo, D.J. Joe, J.H. Han, J.B. Yoon, K.J. Lee, Nanomater. Energy 35 (2017) 415–423.
[34] B. Shi, Z. Li, Y. Fan, Adv. Mater. (2018) e1801511.
[35] W. Jiang, H. Li, Z. Liu, Z. Li, J.J. Tian, B.J. Shi, Y. Zou, H. Ouyang, C.C. Zhao, L.M. Zhao, R. Sun, H.R. Zheng, Y.B. Fan, Z.L. Wang, Z. Li, Adv. Mater. 30 (2018) 1801895.
[36] A. Kumar, K.C. Nune, R.D.K. Misra, Biomater. Sci-Uk 4 (2016) 136–144.
[37] G. Murillo, A. Blanquer, C. Vargas-Estevez, L. Barrios, E. Ibanez, C. Nogues, J. Esteve, Adv. Mater. 29 (2017) 1605048.
[38] C.T. Brighton, W. Wang, R. Seldes, G.H. Zhang, S.R. Pollack, J. Bone Joint Surg. Am. 83a (2001) 1514–1523.
[39] T.W. Balmer, S. Vesztergom, P. Broekmann, A. Stahel, P. Buchler, Sci. Rep-Uk 8 (2018) 8601.
[40] P. Zhou, F. He, Y. Han, B. Liu, S. Wei, Bioelectrochemistry 124 (2018) 7–12.
[41] A.K. Dubey, P. Agrawal, R.D. Misra, B. Basu, J. Mater. Sci. Mater. Med. 24 (2013) 1789–1798.
[42] I.S. Kim, J.K. Song, Y.M. Song, T.H. Cho, T.H. Lee, S.S. Lim, S.J. Kim, S.J. Hwang, Tissue Eng. 15 (2009) 2411–2422.
[43] Q. Zheng, Y. Zou, Y.L. Zhang, Z. Liu, B.J. Shi, X.X. Wang, Y.M. Jin, H. Ouyang, Z. Li, Z.L. Wang, Sci. Adv. 2 (2016) e150147.
[44] R.T. Franceschi, B.S. Iyer, J. Bone Miner. Res. 7 (1992) 235–246.
[45] Y. Liu, X.H. Zhang, C. Cao, Y.L. Zhang, J.Q. Wei, Y.J. Li, W.W. Liang, Z.W. Hu, J.X. Zhang, Y. Wei, X.L. Deng, Adv. Funct. Mater. 27 (2017) 1703771.

Dr. Jingjing Tian received her Ph.D. from Beijing Institute of Nanoenergy and Nanosystem, University of Chinese Academy of Sciences in Department of Physical Chemistry in 2018, and bachelor degree from Yantai University in department of Bioengineering in 2013. Her research work is focusing on the application of nanogenerator on anti-bacterial and self-powered biomedical system.

Dr. Rui Shi is an associate professor of Beijing Jishuitan Hospital (the Fourth Clinical Medical College of Peking University)/Beijing Research Institute of Traumatology and Orthopaedics. She received her Ph.D. in Beijing University of Chemical Technology. She is currently working as the visiting professor at Beijing Institute of Nanoenergy and Nanosystems, Chinese Academy of Science. Her research interests include anti-bacterial technologies and bone regeneration.

Zhuo Liu received the B.E. degree in Medical Imaging from Gannan Medical University in 2014. And received the M.A. degree in Biomedical Engineering from Beihang University, Beijing, China, in 2017. He is current pursuing the Ph.D. degree at Beihang University. His research interests are focusing on self-powered biomedical systems and measurement of cell traction force.

Han Ouyang received the B.S. degree in Material Physics from southwest university of science and technology, China, in 2014. He is current pursuing the Ph.D. degree at Beijing Institute of Nanoenergy and Nanosystems, Chinese Academy of Sciences. His research work is focusing on self-powered sensor systems.

Dr. Min Yu received her Ph.D. degree from Peking University in department of Biomedical Engineering in 2010. Her research work is focus on nanodevices, nanomedicine and biomedical applications of quantum dots.

Chaochao Zhao received the Master and B.E. degree in Chemical Engineering of Hebei University of Science and Technology in 2015 and 2012, respectively. He is currently pursuing the Ph.D. degree in Beijing Institute of Nanoenergy and Nanosystems, Chinese Academy of Sciences. His research work is focusing on self-powered drug delivery systems.

Yang Zou received his bachelor degree from Beihang University in department of bioengineering in 2016. He is currently pursuing the Ph.D. degree in Beijing Institute of Nanoenergy and Nanosystems, Chinese Academy of Sciences. His research interests include self-powered biodegradable biomedical devices and measurement of cell traction force.

Dongjie Jiang received the B.S. degree in Zhejiang Sci-Tech University in the department of light chemical engineering at 2017. He is currently pursuing his M.E. degree in Beijing Institute of Nanoenergy and Nanosystems, Chinese Academy of Sciences. His research focus is nanogenerator and its application in biological signal sensing.

Jingshuang Zhang received her Master degree from Capital Medical University in 2016, and Bachelor degree from Hebei North University in 2013. Her major is biochemistry and molecular biology.

Prof. Zhou Li received his Ph.D. from Peking University in 2010, and bachelor degree from Wuhan University in 2004. Currently, he is a Professor in Beijing Institute of Nanoenergy and Nanosystems, and School of Nanoscience and Technology, University of Chinese Academy of Sciences. Prof. Zhou Li's research interest focused on single cell mechanics, implantable energy harvester and self-powered medical system, including nano-biosensors and nanogenerators.